Lab-on-chip clinorotation system for live-cell microscopy under simulated microgravity

Alvin G. Yew[a], Javier Atencia[b], Ben Chinn[c], Adam H. Hsieh[b]

[a]*Corresponding author:*
NASA Goddard Space Flight Center
Greenbelt, MD 20771, USA
Alvin.G.Yew@nasa.gov
Phone: 301.286.3734

[b]Department of Bioengineering
University of Maryland
College Park, MD 20742, USA

[c]Department of Electrical Engineering
University of Maryland
College Park, MD 20742, USA

Abstract

Cells in microgravity are subject to mechanical unloading and changes to the surrounding chemical environment. How these factors jointly influence cellular function is not well understood. We can investigate their role using ground-based analogues to spaceflight, where mechanical unloading is simulated through the time-averaged nullification of gravity. The prevailing method for cellular microgravity simulation is to use fluid-filled containers called clinostats. However, conventional clinostats are not designed for temporally tracking cell response, nor are they able to establish dynamic fluid environments. To address these needs, we developed a Clinorotation Time-lapse Microscopy (CTM) system that accommodates lab-on-chip cell culture devices for visualizing time-dependent alterations to cellular behavior. For the purpose of demonstrating CTM, we present preliminary results showing time-dependent differences in cell area between human mesenchymal stem cells (hMSCs) under modeled microgravity and normal gravity.

Keywords: space biology; clinorotation; clinostat; live-cell; microscopy; stem cell

1. Introduction

Cellular specimens in spaceflight exhibit abnormal, time-evolving morphology and cytoarchitecture (e.g. cytoskeleton, focal adhesions, etc.), which may affect certain cell events including replication, differentiation, migration, and signaling [1-3]. These events generally confer broader changes to tissues that can lead to reduced bone mineral density [4,5], muscle atrophy [6,7], back pain [8,9], and other ailments [10]. The success of long-duration human space exploration requires countermeasures that address the fundamental cellular changes

adopted in microgravity and are most effective if they consider the underlying dynamic processes driving these alterations.

The National Aeronautics and Space Administration (NASA), European Space Agency (ESA), and other organizations manage a robust portfolio of research initiatives for space biology, using the International Space Station (ISS) as their flagship facility. However, the ISS is not easily accessible and does not often accommodate continuous monitoring of onboard experiments, thereby limiting the ability to observe time-evolving processes. While ground-based microgravity simulations with conventional clinostats [11-13] are notably less expensive, they also preclude the possibility of real-time cell monitoring. State-of-the-art methods do not easily allow time-dependent investigations to identify the mechanisms of cellular alterations and may consequently lead to an incomplete understanding of how microgravity affects human health.

A brute-force remedy for this latent need is to incorporate a full-scale microscope onto a mega-scale clinorotation platform for ground simulations. Clinorotation was initially developed for studying how plants respond to gravity and is currently the prevailing method for cellular microgravity simulation. It is based on the assumption that a time-averaged nullification of gravity can be achieved by reorienting the gravity vector on biological samples, and that the reorientation is fast enough to ensure that specimens cannot perceive a gravitational bias in any direction. The ESA's clinostat microscope [14] is an example of one mega-scale configuration. Another example was published in 2010 by Pache et. al. [15] and was optimized in 2012 by Toy et. al. [16] to demonstrate how digital holographic microscopy (DHM) with mega-scale clinorotation can monitor cytoskeletal changes in simulated microgravity. Interestingly, these studies showed the first published, same-cell images exhibiting time-dependent lamllipodium

65 retraction, filopodia extension, and perinuclear actin accumulation under clinorotation compared
66 to static controls.

67 Even though the clinostat microscope and CR-DHM can be used for time-lapse
68 microscopy, many labs do not have the resources or facility space to incorporate a mega-scale
69 system. Furthermore, mega-scale systems could induce significant mechanical vibrations or
70 impulse loads that may disturb cell cultures. Therefore, we present a clinochip system for
71 Clinorotation Time-lapse Microscopy (CTM) that may also enable long-term, low shear cell
72 culture. While the underlying principles of the clinochip are identical to conventional clinostats,
73 and certainly similar to the mega-scale systems, CTM enables live-cell imaging, without
74 prohibitively large equipment or disruption of culture environments. Importantly, CTM
75 represents a significant step forward in space biology research because it is an affordable, size-
76 manageable system that enables microgravity studies of not only traditional endpoint outcomes,
77 but also dynamic cellular processes.

78 Moreover, CTM is compatible with any lab-on-chip device assembled on a standard
79 microscope slide, for example: microcavites for cell culture; chemical gradient generators; cell
80 sorters; and capillary-based separation columns. It can accommodate cells in monolayer,
81 suspension, and 3D constructs. State-of-the-art microfluidic techniques allow us to precisely
82 modulate microscale flow to create complex cell culture environments, a feature that is not
83 always possible with conventional clinostat devices. Specifically, the surge in microfluidics
84 research in the past decade has enabled exciting new capabilities for probing cells in a variety of
85 ways. This technology can easily be leveraged with CTM.

86 Media exchange between an external reservoir and a rotating "clinochip" platform on
87 CTM is feasible by integrating lab-on-chips with a miniature rotary union for programmable

88 media exchange, continuous media circulation, and chemical infusions. Taken together, the
89 enormous scope of possible microgravity investigations distinguishes clinochips from
90 conventional clinostats. We believe that their affordability, easy implementation, and
91 amenability for live-cell imaging will fully-enable researchers seeking to understand the time-
92 evolution of cellular alterations under microgravity simulation.
93

94 **2. Material and methods**

95 *2.1. CTM system*

96 We fabricated a clinochip system that enables imaging of cells subjected to two-
97 dimensional microgravity simulation and can be operated in parallel with a static chip as a
98 control. The CTM configuration depicted in Fig. 1a uses a stepper motor with a resolution of 200
99 macrosteps per revolution and a two-gear train assembly to transfer rotational motion to a
100 clinochip platform that holds a lab-on-chip device. This rotating platform pivots on a custom-
101 built miniature polyterafluoroethylene (PTFE) rotary joint that allows one rotational degree of
102 freedom about the spin axis. Additionally, the rotary joint is equipped to manage fluid exchange
103 between external fluid reservoirs and devices on the rotating clinochip platform.

104 In brief (refer to Fig. 1b), the rotary joint was fabricated with 19-gauge blunt syringe
105 needle tips that were press-fitted from the rear of CNC-milled PTFE connectors into 1 mm
106 access holes until flush with the microchannel groves on the front. Axially self-aligning
107 neodymium ring magnets (RC86, K&J Magnetics) were pressed into slots at the rear of the
108 connectors and provide substantial clamping force when mating two identical connectors.
109 Commonly used as a material for gaskets, PTFE has some unique properties that also make it
110 suitable for the rotary joint: 1) high compressibility forms a tighter seal at the mating interface;

111 2) hydrophobicity helps to prevent fluid wetting and leakage at the interface; 3) low coefficient
112 of friction allows for easy rotation about the spin axis.
113 Open-loop control is established with LabVIEW (v.10.0, National Instruments) for the
114 stepper motor (HT11-013D, Applied Motion Products), inverted fluorescence microscope (IX81,
115 Olympus Corporation), XY motorized stage (MS-2000, Applied Scientific Instrumentation), and
116 B/W CCD digital camera (ORCA-ER, Hamamatsu Photonics).
117
118 *2.2. Lab-on-chip devices*
119 Live-cell CTM devices were fabricated using a high-frequency corona treater (BD-20AC,
120 Electrotechnic Products) to energetically bond layers of polydimethylsiloxane (Sylgard 184,
121 Dow Corning), i.e. PDMS, at 10:1 ratio of base to curing agent, between 75x25x1 mm glass
122 slides. Geometric features in PDMS were formed by a high-resolution razor cutter (FC8000,
123 Graphtec). To prepare microfluidic devices for experiments, cell culture surfaces, consisting of a
124 200 micron tall by 1 mm wide microchannel constructed from PDMS and glass, were cleaned
125 with 70% ethanol, rinsed in deionized water, and air-dried. Immediately before cell experiments,
126 the microchannel was incubated in ambient for one hour with 15 ug/mL fibronectin (354008, BD
127 Sciences) in phosphate buffer saline (PBS) without Ca++ and Mg++ and then gently rinsed 2-3
128 times with PBS. Fibronectin-treated surfaces were kept hydrated by filling culture cavities with
129 fresh PBS and were sterilized by ultraviolet exposure for 15 minutes prior to cell seeding.
130
131 *2.3. Cell culture experiments*
132 Passage-5 hMSCs were expanded in 6-well plates with hMSC media until confluent.
133 Stem cells were trypsinized, centrifuged, resuspended at 10^5 cells/mL, plated into microchannels,

134 and incubated in a microscope-amenable environmental chamber (Precision Plastics) at 37 °C,
135 50% humidity, and 5% CO_2 for 20 min before microchannels were gently flushed with hMSC
136 media to remove non-adherent cells. One clinochip and one static chip were placed onto the
137 CTM system, which was mounted to an XY motorized stage (MS-2000, Applied Scientific
138 Instrumentation) on an inverted fluorescence microscope (IX81, Olympus Corporation).
139 A group of cells that had been seeded on both the clino- and static chip were randomly
140 selected for time-lapse microscopy using differential interference contrast (DIC) and phase
141 contrast. Both chips had similar seeding densities, roughly 5-6 cells in the field of view using a
142 10X objective, and similar initial morphologies. Before we subjected the clinochip to 60 RPM
143 clinorotation, we acquired an initial image of both chips at 0 hrs. At each subsequent hour, for
144 8 hrs, we acquired additional images. Figure 2 shows same-cell images at 0, 1, 4, and 8 hr time
145 points for 60 and 0 RPM.
146
147 **Results**
148 From these timelapse images, we measured time-evolving, same-cell areas using a
149 custom Matlab algorithm (see Fig 3). Average areas were not different in the first 3 hrs of
150 clinorotation. After 5 hrs however, cell areas at 0 RPM increased dramatically while cells at
151 60 RPM showed little change. Significant differences were found at 6-8 hr time points.
152 Moreover, at each time point, we conducted a visual inspection of other cell groups and found
153 that morphologies for the randomly selected cells were qualitatively representative of the entire
154 population in the chip. Although our sample size was small, our preliminary CTM results
155 demonstrate evidence of substantial changes to hMSC morphology that may affect other
156 functions important to bone health including differentiation and chemotactic homing.

157 We also took measurements for the absolute difference of same-cell areas between each
158 time point and the previous point, as shown in Fig. 4. While much variability exists in the data,
159 specimens at 0 RPM were measured at approximately 70% higher average difference when
160 compared with 60 RPM.
161

162 **Discussion**

163 The goal of this paper was to present a way to improve on state-of-the-art clinorotation
164 devices. Since particle physics in conventional clinostats is impossible to accurately control in
165 experiments, cells can be subjected to mechanical forces and chemical gradients that might not
166 be physiological. Additionally, adherent cells in these clinostats need to be seeded on
167 microcarrier beads that have limited surface area for proliferation, which prohibits long-term
168 culture. Moreover, the constant movement of cells through culture media makes dynamic
169 bioassays, which are important for a more holistic understanding of cellular response, generally
170 unattainable. Finally, without the ability to manipulate culture conditions, for example, by
171 modulating the chemical microenvironment, conventional clinostats can only offer a narrow
172 range of possible science investigations.

173 In conjunction with lab-on-chip technologies, the CTM methods described in this paper
174 addresses these issues and may enable a wide range of live-cell, time-dependent investigations in
175 simulated microgravity. As a whole, CTM allowed us to identify the time-evolution of cell
176 response in simulated microgravity without the limitation of only being able to obtain images at
177 static time-points that are usually the extent of the capabilities afforded by conventional clinostat
178 devices. Using static time points would limit the ability to understand how the time-dosage of
179 microgravity affects cells, introduces more variability in experimental data, and may require

180 more experimental controls to rule out confounding factors than our CTM system. For these
181 reasons, and for its affordability and versatility, we believe that CTM represents a significant
182 step forward in space biology research.

183 Our preliminary experiments examine early spreading in hMSCs, when cells are only
184 loosely attached and could mimic how daughter cells in mitosis may behave in microgravity. We
185 hypothesize that microgravity-induced morphological alterations may also affect lineage
186 commitment and may be responsible for the markedly lower rates of differentiation observed in
187 stem cells flown in space [17]. This hypothesis warrants further study, but agrees with previously
188 published work showing that simulated microgravity disrupts hMSC function by enhancing
189 adipogenesis and reducing osteoblastogenesis [18,19]. In future work, we will use CTM to
190 understand how microgravity may affect early attachment by fluorescently tagging cytoskeletal
191 elements and correlating cell morphology with long-term rates of proliferation.

192 Studying hMSCs is particularly useful because they are important for maintaining bone
193 health and play an integral role in bone fracture healing. Normal cell functions are hypothesized
194 to be adversely affected in spaceflight and may partially explain the decreased bone health and
195 generally poor quality of fracture healing in animal models flown in space. The incomplete
196 understanding of hMSC behavior, as related to bone health in space, may jeopardize the success
197 of future, long-duration manned missions; however, CTM provides a way to improve our
198 understanding.

199 While CTM is a powerful tool for space biologists, the design that we've presented can
200 only be used to simulate microgravity in 2D, i.e. one axis of rotation. Although this is not
201 considered a major hurdle in microgravity research, as other investigators still use 2D clinostats,
202 3D microgravity simulation through random positioning machines may be a superior model for

203 microgravity. In order to achieve 3D clinorotation on a microscope stage-amenable platform,
204 clinochip devices would need to be significantly reduced in size. Also, a completely new type of
205 rotary joint would need to be designed to accommodate the additional axis of rotation. These
206 design limitations can also be considered for future work.

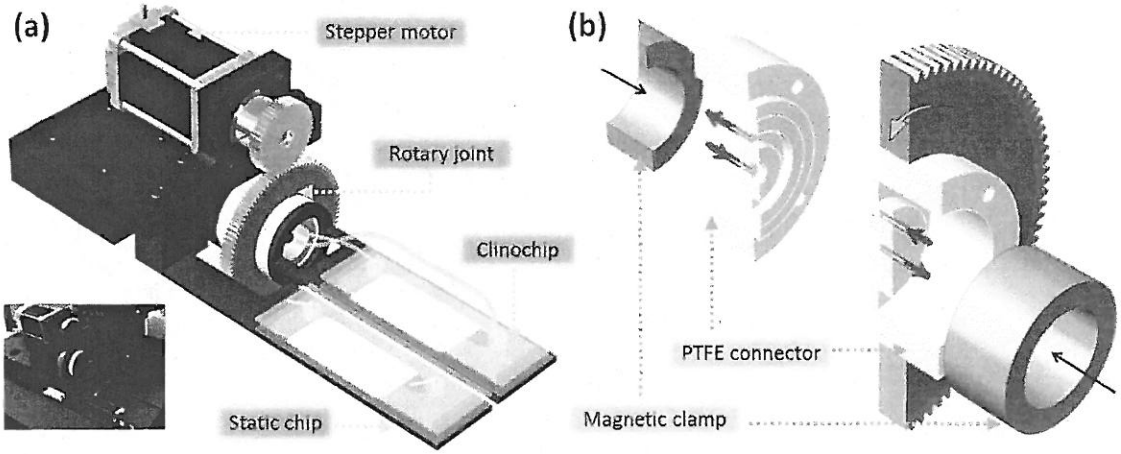

Figure 1. Microscope stage-amenable, Clinorotation Time-lapse Microscopy (CTM) system enables live-cell imaging of cells. (a) CTM components include a clinochip for simulated microgravity and static chip for a 1-g static control. (b) exploded computer model of rotary union designed to allow media perfusion into clinochips for long-term cell culture.

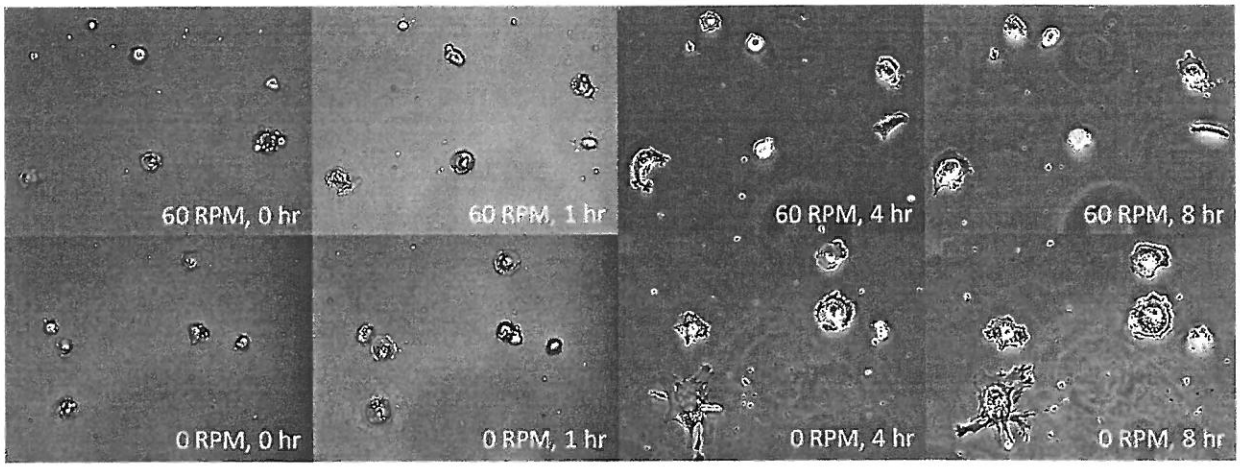

Figure 2. Time-evolution of early spreading in hMSCs imaged under DIC and phase contrast at 60 RPM clinorotation and at 0 RPM static control. Cells at 0 RPM were more spread at 4-8 hrs compared to 60 RPM.

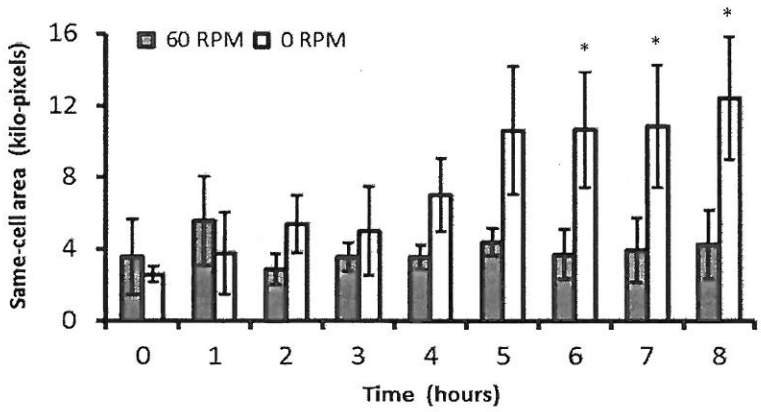

Figure 3. Mean values of same-cell areas (n=3) and 1 S.D. error bars. From calculated cell areas at 8 hrs (based on images from Fig 2), cells with the three median values were digitally-tagged. To eliminate outliers in cell behavior, only the tagged cells were then used to calculate areas at all remaining time points and used for comparison of means. * $p<0.05$ difference in cell area between the 60 and 0 RPM chips.

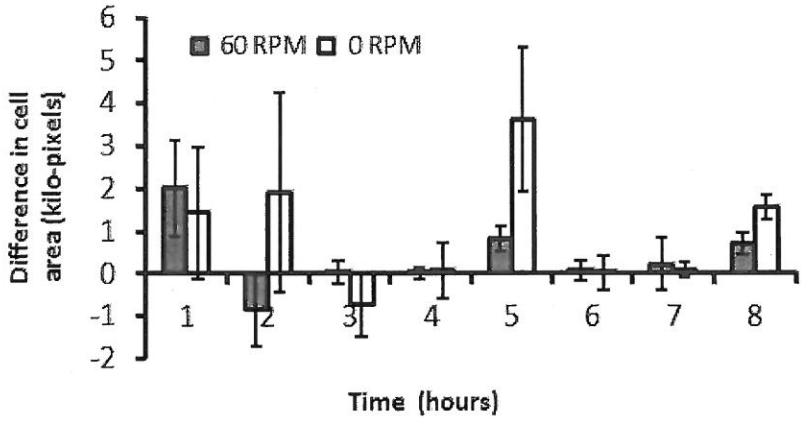

227

228 **Figure 4.** Difference in cell area between current time point and previous time point (n=3) and

229 1 S.D. error bars. To eliminate outliers in cell behavior, only the 3 median values of difference

230 were used for analysis. Specimens at 0 RPM averaged 70% higher differences when compared

231 with 60 RPM.

232 **References**

233

234 [1] D.H. Slentz, G.A. Truske, W.E. Kraus, Effects of chronic exposure to simulated
235 microgravity on skeletal muscle cell proliferation and differentiation, In Vitro Cell Dev Biol
236 Anim, 37(3) (2010) 148-156.

237

238 [2] K. Hirasaka, T. Nikawa, L. Yuge, I. Ishihara, A. Higashibata, N. Ishioka, A. Okubo, T.
239 Miyashita, N. Suzue, T. Ogawa, M. Orada, K. Kishi, Clinorotation prevents differentiation
240 of rat myoblastic L6 cells in association with reduced NF-κB signaling, Biochim Biophys
241 Acta, 1743(1) (2005) 130-140.

242

243 [3] C. Ontiveros, L.R. McCabe, Simulated microgravity suppresses osteoblast phenotype,
244 Runx2 levels and AP-1 transactivation, J Cell Biochem, 88(3) (2002) 427-437.

245

246 [4] L. Vico, P. Collet, A. Guignandon, M.H. Lafage-Proust, T. Thomas, M. Rehailia, C.
247 Alexandre, Effects of long-term microgravity exposure on cancellous and cortical weight-
248 bearing bones of cosmonauts, Lancet, 355(9215) (2000) 1607-1611.

249

250 [5] A.D. Leblanc, V.S. Schneider, H.J. Evans, D.A. Engelbretson, J.M. Krebs, Bone mineral
251 loss and recovery after 17 weeks of bed rest. J Bone Miner Res, 5(8) (2009) 843-850.

252

253 [6] A. LeBlanc, V. Schneider, L. Shackelford, S. West, V. Oganov, A. Bakulin, L. Voronin,
254 Bone mineral and lean tissue loss after long duration space flight. J Musculoskelet Neuronal
255 Interact, 1(2) (2000) 157-60.
256
257 [7] S. Gupta, S.L. Manske, S. Judex, Increasing the number of unloading/reambulation cycles
258 does not adversely impact body composition and lumbar bone mineral density but reduces
259 tissue sensitivity. Acta Astronaut (2012), in press.
260
261 [8] J.V. Sayson, A.R. Hargens, Pathophysiology of low back pain during exposure to
262 microgravity. Aviat Space Environ Med, 79(4) (2008) 365-373.
263
264 [9] S.L. Johnston, M.R. Campbell, R. Scheuring, A.H. Feiveson, Risk of herniated nucleus
265 pulposus among US astronauts. Aviat Space Environ Med, 81(6) (2010) 566-574.
266
267 [10] R.A. Scheuring, C.H. Mathers, J.A. Jones, M.L. Wear, Musculoskeletal injuries and minor
268 trauma in space: incidence and injury mechanisms in US astronauts. Aviat Space Environ
269 Med, 80(2) (2009) 117-124.
270
271 [11] D.M. Klaus, Clinostats and bioreactors. Gravit Space Biol Bull, 14(2) (2007) 55-64.
272
273 [12] M. Cogli, The fast rotating clinostat: a history of its use in gravitational biology and a
274 comparison of ground-based and flight experiment results, Gravit Space Biol Bull, 5(2)
275 (1992) 59-67.

276

277 [13] J.J. van Loon, Some history and use of the random positioning machine, RPM, in gravity
278 related research, Adv Space Res, 39(7) (2007) 1161-1165.

279

280 [14] European Space Agency. DLR – Clinostats, centrifuges, RPM. Human spaceflight research.
281 Retrieved December 20, 2012, from
282 http://www.esa.int/Our_Activities/Human_Spaceflight/Human_Spaceflight_Research/DLR_
283 -_Clinostats_Centrifugues_RPM

284

285 [15] C. Pache, J. Kühn, K. Westphal, M.F. Toy, J. Parent, O. Büchi, A. Franco-Obregón, C.
286 Depeursinge, M. Egli, Digital holographic microscopy real-time monitoring of
287 cytoarchitectural alterations during simulated microgravity, J Biomed Opt, 15(2) (2010)
288 026021-026021.

289

290 [16] M.F. Toy, S. Richard, J. Kühn, A. Franco-Obregón, M. Egli, C. Depeursinge, Enhanced
291 robustness digital holographic microscopy for demanding environment of space biology,
292 Biomed Opt Express, 3(2) (2012) 313-326.

293

294 [17] H. Finkelstein, N. Dvorochkin, R. Yousuf, R.K. Globus, E.A. Almeida, Spaceflight Reduces
295 the Tissue Regenerative Potential of Stem Cells by Decreasing Proliferation and Increasing
296 Early Differentiation. Stem Cells Biology Poster Session. 50th Annual Meeting of the
297 American Society for Cell Biology, Philadelphia, PA, December 11-15, 2010.

298

299 [18] M. Zayzafoon, W.E. Gathings, J.M. McDonald, Modeled microgravity inhibits osteogenic
300 differentiation of human mesenchymal stem cells and increases adipogenesis.
301 Endocrinology, 145(5) (2004) 2421-2432.
302
303 [19] V.E. Meyers, M. Zayzafoon, J.T. Douglas, J.M. McDonald, RhoA and cytoskeletal
304 disruption mediate reduced osteoblastogenesis and enhanced adipogenesis of human
305 mesenchymal stem cells in modeled microgravity. J Bone Miner Res, 20(10) (2005) 1858-
306 1866.